substance: boron compounds with group IV elements: boron carbide
property: details of structure

Unit cell in Fig. 1 (see also Fig. 2)

Structure: rhombohedral
Space group: $D_{3d}^5 - R\,\bar{3}\,m$;

This characterization of an idealized boron carbide structure must not be misunderstood. In reality, at no composition within the homogeneity range a specific elementary cell for the whole volume can be described. At any composition the structure consists of a statistical arrangement of differently structured cells, whose only agreement is the arrangement of 12 atoms in a distorted icosahedron at the vertex of the rhombohedral cell (B_{12} icosahedra and $B_{11}C$ icosahedra with the C atom statistically substituting for boron at one of the six so called polar sites), and, in most cases, three atoms forming a largely covalently bonded chain (within the detection limit C-B-C and C-B-B only) on the main diagonal of the rhombohedral cell. At the carbon-rich limit of the homogeneity range ($B_{4.3}C$), nearly all cells contain such three-atom chains. However, with decreasing carbon content an increasing number of cells is free of such chains. This number reaches about 50 % close to the boron-rich limit of the homogeneity range. It is not definitely clear, what the missing of the chain means. Two versions seem possible: (i) α-rhombohedral boron-like unit cells, (ii) two unbounded B atoms at the end positions of the chain such saturating the outer bonds of the so called equatorial atoms of the icosahedra. While in the analysis of phonon spectra both alternatives could not be distinguished [92K2, 92K1, 94K1, 94K2], the calculation of reaction kinetics clearly favors the second model [96K1] (cited also in [98R]). By neutron diffraction the vacancies of the central B(3) were determined [96K2].

The assumption of B_4 planes in the unit cell of boron carbide [75Y, 73Y, 86Y] (Fig. 3) has lateron not been confirmed by other authors.

Structure formula: $(B_{12})_x(B_{11}C)_{1-x}(CBC)_m(CBB)_n$ ($m+n \leq 1$) or more probably

$(B_{12})_x(B_{11}C)_{1-x}(CBC)_m(CBB)_n(CCC)_o(B\square B)_p$ ($m+n+o+p = 1$; for $B_{4.3}C$ o, p = 0)

It must be paid attention to the fact that all hitherto performed theoretical calculations on boron carbide (see below) are based on idealized structures like B_4C ($(B_{12})CCC$ and $(B_{11}C)CBC$ respectively) or $B_{13}C_2$ ($(B_{12})CBC$ and $(B_{11}C)CBB$, respectively) and don't take the structural variety into account.

Concentration of the structural elements (B_{12} and $B_{11}C$ icosahedra, C-B-C and C-B-B chains) in the rhombohedral unit cells and the share of chainless unit cells depending on the carbon content in Fig. 4 [92K2, 92K1, 94K1, 94K2].

Density of the chain-free unit cells depending on the carbon content from analysis of the phonon spectra [92K2, 92K1, 94K1, 94K3], from the correlation between structural defects and valence electron deficiency [99S1, 99S2, 99W] and vacancies of the central B(3) atom derived from neutron diffraction in Fig. 5 [96K2].

High resolution imaging of boron carbide microstructures [86M].

Occupation density of interstitial B(6) sites away from the central B(3) site depending on the carbon content in Fig. 6 [95M] (For more details see below (neutron diffraction).

Further references on the boron carbide structure: [59S, 66S, 70A, 71H, 75Y, 73Y, 77M2, 77M1, 76M, 71K, 76W1, 76W2, 78H, 81B1, 81B2, 81W, 79K1, 79K2, 80K].

unit cell parameters

Rhombohedral unit cell of boron carbide with interatomic bond lengths indicated for some selected compositions in Fig. 7 (=2) [91A].

unit cell: Fig. 8, C – B – C chain: Fig. 3a, B_4 plane: Fig. 3b, icosahedron: Fig. 3c.

For morphology of boron carbide single crystals, see [71S]. For dislocation nodes, see [72A, 73A, 75A, 75L].

B_4C (probably better $B_{4.3}C$ = carbon-rich limit of the homogeneity range).

lattice parameter

a	5.6039(4) Å	hexagonal presentation	87L
c	12.0786(14) Å		
c/*a*	2.16		91L
V	328.5 Å^3		

interatomic distances
(in Å)

d	1.72	inter-icosahedral	91L
	1.79	intra-icosahedral	
	1.68	origin to 6 B(1)	
	1.73	origin to 6 B(2)	
	1.43	X – B in X – B – X (chain)	
	1.61	X – 3 B(1)	

structure refinement of a crystal with *a* = 5.60124 Å and *c* = 12.0734(13) Å (consistent with a B_4C (probably better $B_{4.3}C$) composition) [87M]

Atom	*x*	*z*	U_{11}	U_{33}	U_{12}
B(1)	0.16303(3)	0.35838(3)	41(1)	59(1)	21(1)
B(2)	0.10741(3)	0.11391(3)	45(1)	63(1)	22(1)
B(3)	0	0.5	76(2)	60(3)	38(1)
C	0	0.38126(4)	40(1)	49(2)	20(1)

$y = -x$; $U_{22} = U_{11}$, U_{ij} (x 10^{-4}) Å^2

$B_{13}C_2$

lattice parameters

rhombohedral presentation

a	5.198(2) Å	*T* = 300 K	X-ray diffraction	79K1
α	65.62°			

hexagonal presentation

a	5.633(1) Å	*T* = 300 K	X-ray diffraction	79K1,
c	12.164(2) Å			79K2

Dependence of lattice parameters on C content: Fig. 9.

c/*a*	2.16		91L
V	334.3 Å^3		

interatomic distances
(in Å)

d	1.73	inter-icosahedral	91L
	1.80	intra-icosahedral	
	1.69	origin to 6 B(1)	
	1.74	origin to 6 B(2)	
	1.43	X – B in X – B – X (chain)	
	1.62	X – 3 B(1)	

quadrupole coupling constants

ν_{Qa}	520(30) kHz	NMR	71H
ν_{Qb}	30 kHz	NMR	

$B_{9.3}C$

lattice parameters

a	5.620(1) Å		75Y
c	12.1428(2) Å		
c/*a*	2.15		86Y
V	338.2 $Å^3$		91L

interatomic distances

(in Å)

d	1.74	inter-icosahedral	91L
	1.80	intra-icosahedral	
	1.70	origin to 6 B(1)	
	1.73	origin to 6 B(2)	
	1.44	X – B in X – B – X (chain)	
	1.63	X – 3 B(1)	

Boron carbides. Results of chemical and X-ray analysis [91G]

No.	Chemical analysis [wt.%]			free C	Hexagonal cell parameters (Å)		Rhomb. cell volume	Rhombohedral cell parameters	
	total B	total C	at.% C	wt.%	*a*	*c*	Å^3	*a* [Å]	α [°]
1504	87.52 ± 0.74	8.67 ± 0.10	8.19 ± 0.l5	-	5.6408 ± 8.3E-3	12.1597 ± l.9E-2	111.690 ± 0.500	5.l995 ± 7.3E-3	65.699 ± l.4E-1
1593	85.92 ± 0.08	9.38 ± 0.90	8.95 ± 0.79	-	5.6414 ± 2.3E-3	12.1786 ± 9.5E-3	111.887 ± 0.177	5.2046 ± 3.0E-3	65.634 ± 5.3E-2
1658	86.65 ± 0.47	10.01 ± 0.05	9.42 ± 0.09	-	5.6448 ± 2.1E-3	12.1720 ± 5.2E-3	111.961 ± 0.130	5.2042 ± l.9E-3	65.686 ± 3.6E-2
815	89.68 ± 0.20	10.93 ± 0.09	9.88 ± 0.09	-	5.6417 ± 2.0E-3	12.1748 ± 5.0E-3	111.864 ± 0.125	5.2038 ± 1.9E-3	65.651 ± 3.4E-2
1588	85.47 ± 0.01	10.80 ± 0.53	10.21 ± 0.45	-	5.6310 ± l.3E-3	12.1928 ± 5.3E-3	111.605 ± 0.101	5.2046 ± 1.7E-3	65.499 ± 3.0E-
1599	84.11 ± 0.22	10.90 ± 0.89	10.45 ± 0.79	-	5.6377 ± 6.5E-4	12.1690 ± 2.4E-3	111.652 ± 0.048	5.2008 ± 8.0E-4	65.640 ± l.4E-2
1609	83.05 ± 0.11	11.32 ± 0.10	10.93+0.10	-	5.6210 ± l.3E-3	12.2148 ± 3.8E-3	111.410 ± 0.085	5.2067 ± l.3E-3	65.338 ± 2.4E-
1595	81.31 ± 0.01	12.56 ± 0.54	12.21 ± 0.46	-	5.6230 ± 9.9E-4	12.1811 ± 2.7E-3	111.181 ± 0.064	5.1986 ± 9.8E-4	65.478 ± 1.8E-2
1366	83.70 ± 0.31	14.82 ± 0.20	13.75 ± 0.20	-	5.6216 ± l.3E-3	12.1726 ± 5.9E-3	111.048 ± 0.106	5.l959 ± 1.9E-3	65.498 ± 3.2E-2
1503	81.60 ± 0.71	14.77 ± 0.30	14.01 ± 0.35	-	5.6147 ± l.1E-3	12.1848 ± 3.6E-3	110.887 ± 0.078	5.1966 ± l.3E-3	65.398 ± 2.2E-2
1365	82.49 ± 0.07	15.54 ± 0.33	14.50 ± 0.27	-	5.6133 ± l.2E-3	12.1751 ± 4.5E-3	110.744 ± 0.087	5.1936 ± l.5E-3	65.423 ± 2.6E-2
1587	82.07 ± 0.12	16.51 ± 0.64	15.33 ± 0.52	-	5.6139 ± 7.1E-4	12.1513 ± 2.5E-3	110.551 ± 0.051	5.1876 ± 8.4E-4	65.515 ± l.5E-2
1913	81.37 ± 0.13	16.68 ± 0.06	15.58 ± 0.07	-	5.6143 ± l.0E-3	12.1428 ± 4.7E-3	110.489 1 0.083	5.1855 ± l.5E-3	65.550 ± 2.6E-2
1420	79.81 ± 0.03	17.70 ± 0.10	16.64 ± 0.08	-	5.6058 ± 4.6E-4	12.1299 ± 2.3E-3	110.038 ± 0 039	5.1791 ± 7.1 E-4	65.530 ± 1.2E-
1911	79.34 ± 0.33	18.07 ± 0.02	17.01 ± 0.07	-	5.6039 ± 9.1 E-4	12.1205 ± 3.4E-3	109.878 ± 0.066	5.1760 ± 1.1 E-3	65.549 ± 2.0E-2
1906	77.35 ± 0.21	19.38 ± 0.02	18.40 ± 0.06	-	5.6023 ± 8.3E-4	12.0960 ± 3.1E-3	109.593 ± 0.061	5.1690 ± 1.0E-3	65.627 ± 1.8E-2
1908	77.22 ± 0.13	20.20 ± 0.01	19.06 ± 0.03	-	5 5999 ± 9.7E-4	12.0764 ± 4.7E-3	109.322 ± 0.080	5.1631 ± 1.4E-3	65.681 ± 2.5E-2
1812	76.31 ± 0.18	20.84 ± 0.02	19.91 ± 0.08	+2% BN	5.5992 ± 6.4E-4	12.0754 ± 2.1E-3	109.287 ± 0.044	5.1626 ± 7.1E-4	65.679 ± l.3E-2
4597		20.04 ± 0.20		0.04	5.5986 ± 2.4E-3	12.0750 ± 4.9E-3	109.259 ± 0.137	5.1622 ± 2.0E-3	65.676 ± 3.7E-2
1813	76.69 ± 0.15	20.88 ± 0.01	20.05 ± 0.04	+4% BN	5.5994 ± 4.5E-4	12.0752 ± l.9E-3	109.292 ± 0.034	5.1626 ± 5.9E-4	65.682 ± l.1E-2
4593		20.12 ± 0.20		0.12	5.5980 ± 6.5E-4	12.0760 ± 2.8E-3	109.244 ± 0.051	5.1623 ± 8.9E-4	65.667 ± 1.6E-2
4594		20.22 ± 0.20		0.22	5.5979 ± l.4E-3	12.0721 ± 3.1E-3	109.205 ± 0.083	5.1612 ± l.2E-3	65.681 ± 2.3E-2
1902	75.64 ± 0.20	21.36 ± 0.02	20.26 ± 0.06	1.36	5.5985 ± 1.1 E-3	12.0690 ± 4.2E-3	109.200 ± 0.079	5.1606 ± 1.4E-3	65.697 ± 2.4E-2
1904	75.55 ± 0.10	21.81 ± 0.01	20.62 ± 0.03	1.81	5.5986 ± 5.0E-4	12.0696 ± 2.5 E-3	109.210 ± 0.042	5.1608 ± 7.7E-4	65.696 ± 1.3E-2
4818		20.74 ± 0.20		0.74	5.5986 ± 3.9E-4	12.0738 ± l.lE-3	109.248 ± 0.025	5.1619 ± 3.9E-4	65.680 ± 7.2E-3
768		20.94 ± 0.20		0.94	5.5981 ± 8.8E-4	12.0694 ± 2.7E-3	109.188 ± 0.058	5.1606 ± 9.3E-4	65.693 ± 1.7E-2
1810	74.82 ± 0.40	22.70 ± 0.05	21.45 ± 0.13	2.08	5.5988 ± 5.3E-4	12.0734 ± 1.5E-3	109.251 ± 0 034	5.1619 ± 5.2E-4	65.683 ± 9.6E-3
1860	74.05 ± 0.11	22.56 ± 0.05	21.52 ± 0.06	2.56	5.5982 ± 7.5E-4	12.0693 ± 2.5E-3	l09.191 ± 0.052	5.1606 ± 8.6E-4	65.694 ± l.5E-2
4595		22.12 ± 0.20		2.12	5.5960 ± 8.0E-4	12.0670 ± 2.0E-3	109.085 ± 0 049	5.1592 ± 7.5E4	65.685 ± 1.4E-2
4596		22.24 ± 0.20		2.24	5.5982 ± l.4E-3	12.0725 ± 3.1E-3	109.220 ± 0.081	5.1614 ± l.2E-3	65.682 ± 2.2E-2
1836	73.09 ± 0.28	23.63 ± 0.02	22.54 ± 0.08	3.45	5.5980 ± 6.9E-4	12.0689 ± 3.2E-3	109.180 ± 0.056	5.1604 ± 9.9E-4	65.694 ± 1.7E-2
1811	73.85 ± 0.10	24.14 ± 0.02	22.73 ± 0.04	4.76	5.5988 ± 6.4E-4	12.0729 ± l.8E-3	109.247 ± 0.041	5.1618 ± 6.4E-4	65.685 ± l.2E-2
1858	71.81 ± 0.03	24.97 ± 0.02	23.84 ± 0.02	4.97	5.5985 ± 6.4E-4	12.0685 ± 3.3E-3	109.196 ± 0 054	5.1605 ± 9.9E-4	65.699 ± 1.7E-2
1834	71.79 ± 0.24	25.91 ± 0.02	24.52 ± 0.08	5.91	5.5983 ± 8.2E-4	12.0686 ± 3.1 E-3	109.189 ± 0.060	5.1605 ± 1.0E-3	65.697 ± 1.8E-2

Lattice parameters of boron carbide between 8.19 and 24.52 at. % carbon in Fig. 10...12 and special table [91G, 81B1].

Inverted-molecular compression in boron carbide [95N]. Comparison of unit cell volume and icosahedral volume depending on pressure in Fig. 13 [95N].

"Thermal factors" of the different sites in the unit cell in Fig. 14 [91A]. This term is misunderstanding, because in reality it is not only determined by the thermal motion of the atoms but essentially by the statistical distribution of the atoms in the differently structured cells. Hence the "thermal parameters" of the chain atoms increases considerably with decreasing carbon content because of the exchange of C – B – C chains by C – B – B chains [91M] and by the formation of chainfree cells (see Fig. 4) [92K1].

Structure parameter of the unit cell close to the carbon-rich limit of the homogeneity range [94K1, 94W2]

Compound	C content [at. %]	B_{12} icosahedra [%]	$B_{11}C$ icosahedra [%]	*c* [Å]	*a* [Å]	$\Delta c/\Delta a$
$B_{4.3}C$	18.87	0	100	12.075	5.602	
$B_{6.3}C$	13.7	43	57	12.167	5.623	
Difference	5.17	43	43	–0.092	–0.021	4.38

Structure parameter of the icosahedron close to the carbon-rich limit of the homogeneity range [94K1, 94W1]
h: height of icosahedron

Compound	C content [at. %]	Reference	*h* [Å]	$d_{equatorial}$ [Å]	$(\Delta c)_{icos.exp.}$ [Å]	$(\Delta a)_{icos.exp.}$ [Å]	$(\Delta c/\Delta a)_{icos.exp.}$
$B_{4.3}C$ nominal B_4C	20	91A	2.6987	3.2554	#	#	#
$B_{5.3}C$	16	91A	2.7120	3.2707	0.0133	0.0153	0.87
$B_{6.3}C$	13	79K2, 86W	2.7117	3.2773	0.0130	0.0219	0.59
Difference (average)					0.01315	0.0186	0.71

Change of the structural parameters of boron carbide in the case of the substitution of one C atom for B in the icosahedron [94K1] (compared with β-rhombohedral boron (see LB "Boron").

Structure	Element	Δc [Å]	Δa [Å]	$\Delta c/\Delta a$
boron carbide	unit cell	0.214	0.049	4.38
	icosahedron	0.031	0.043	0.71
	difference	0.183	0.006	30.5
β-rhombohedral boron	unit cell and icosahedron	0.032	0.021	1.52

Conclusion: In contrast to β-rhombohedral boron (see LB III/41C), the distortion of the icosahedron $\perp c$ in boron carbide is essentially caused by other effects but the substitution of C for icosahedral B atoms [94W1, 94W2].

further X-ray diffraction results on boron carbide:

Further results on lattice parameters of B_4C ($B_{4.3}C$) boron carbide in [92A1, 94L].

Lattice constants and interatomic distances in [92A2].

Variation of the interatomic distances in boron carbide based on results of different authors in [86C].

Hexagonal lattice constants depending on composition in [91H] and [94W1].

c/*a* relation in the homogeneity range of boron carbide depending on the carbon content in [94K1].

From the analysis of the site occupancies was concluded that the C atoms in the icosahedra substitute for polar B(2) sites [91M].

Comments concerning the crystal structure of B_4C [86L].

neutron diffraction

Lattice parameters (obtained by neutron diffraction compared with those obtained by X-ray diffraction) in [96K2].

Neutron powder diffraction refinement of boron carbides. Nature of intericosahedral chains [95M].

Unlike X–ray diffraction studies neutron diffraction refinements [95M] show significant densities at interstitial sites B(6) away from the chain center B(3). The concentrations of these interstitials are consistent with having one such interstitial for each vacancy at the chain center B(3). Occupancy of B(6) depending on the carbon content in Fig. 5 [95M].

NMR

^{13}C MAS NMR data for isotopically enriched boron carbide. Error of chemical shifts ≤ 0.3 ppm, of larger peak areas 2 %, for small peak areas (< 1% relative intensity) factor 2 [91K].

Compound	C content [at. %]	Chem. shift [ppm]	Rel. intensity	
B_4C *)	18.8	101.3	1.7	91K
		81.9	31.4	
		1.0	66.0	
$B_{13}C_2$	13.33	101.1	< 0.5	
		83.2	8.4	
		67.7	0.5	
		5.4	87.6	
		– 16.4	3.5	
B_9C	10	82.3	1.6	
		66.1	0.4	
		5.8	94.5	
		–16.8	3.5	

*) According to the carbon content, the nominal compound B_4C should be better attributed to the carbon-rich limit of the homogeneity range $B_{4.3}C$.

Variation of ^{13}C and ^{11}B MAS NMR chemical shifts and peak width in Fig. 15 [91K].

NMR spectra of ^{13}C in $B_4{}^{13}C$ and $B_{8.8}{}^{13}C$ and ^{11}B in B_4C in [86C].

The possibility of vacancies in the three-atom chain are mentioned in [86C].

NMR studies of borates and borides (boron carbide included) in [86B].

NMR ^{13}C spin echo intensity compared with calculated results for different structure models in [86A, 86D].

Detailed comparison of numerous compounds with similar chain arrangements; Spectra of ^{13}C NMR with magic angle spinning of B_9C and $B_{12}C_3$ in [86D].

Compositional variation of ^{13}C and ^{11}B MAS NMR chemical shifts and peak breadths in [91K].

Remark to Figs. 4 and 5 Boron carbide: The results shown in Fig. 4 are based on the assumption that the existence of CCC chains aside of CBC and CBB chains in boron carbide can be excluded, because the IR phonon spectra ([92K1, 92K2, 94K1, 94K2]) did not exhibit any absorption band, that could be reasonably attributed to CCC chains. A weak band at about 1430 cm^{-1} that only accidentally occurred in some few spectra was assumed to originate from occasional impurities or defects and therefore was not considered. Recent investigations on isotope-enriched boron carbide confirmed this conclusion for the composition $B_{4.3}C$ only, irrespective of the kind of isotope enrichment. However, in the case of isotope-enriched boron-rich boron carbides obtained by the same kind of preparation, weak but reproducible absorption bands at resonance frequencies between about 1410 and 1450 cm^{-1} and between about 365 and 390 cm^{-1} occurred (see table). These phonon bands were attributed to the stretching mode and the bending mode of CCC chains respectively [99W]. Obviously, depending on the specific conditions of preparation, which however cannot be specified at present, boron-rich boron carbide with and without CCC chains can be obtained. It seems that the results shown in Fig. 5 represent the maximum concentrations of CCC chains that are possible in boron-rich boron carbides. The mentioned accidental phonon bands at 1430 cm^{-1}, that unsystematically vary in occurrence and strength indicate that, depending on the conditions of preparation, any CCC concentration below the limits in Fig. 5 seems possible. The lowest possible CCC concentration is zero, that leads to the concentrations of structural elements shown in Fig. 4 [99W].

References:

59S Silver, A. H., Bray, P. J.: J. Chem. Phys. 31 (1959) 247.
66S Sullenger, B., Kennard, Ch. L.: Sci. Am. 215 No. 7 (1966) 96.
70A Amberger, E., Drumiuski, M., Ploog, K.: J. Less-Common Met. 23 (1971) 43.
71H Hynes, T. V., Alexander, M. N.: J. Chem. Phys. 54 (1971) 5296.
71K Kieffer, R., Gugel, E., Leimer, G., Ettmayer, P.: Ber. Dtsch. Keram. Ges. 48 (1971) 385.
71S Sugaya, T., Watanabe, O.: J. Less-Common Met. 26 (1972) 25.
72A Ashbee, K. H. G., DuBose, C. K. H.: Acta Metall. 20 (1972) 241.
73A Ashbee, K. H. G., Frank, F. C., DuBose, C. K. H.: J. Nucl. Mater. 48 (1973) 193.
73Y Yahel, H. L.: J. Appl. Crystallogr. 6 (1973) 471.
75A Ashbee, K. H. G., Frank, F. C.: J. Nucl. Mater. 55 (1975) 116.
75L Leitnaker, J. M., Stiegler, J. O.: J. Nucl. Mater. 55 (1975) 113.
75Y Yakel, H. L.: Acta Crystallogr. B 31 (1975) 1797.
76M Matkovich, V. I.: J. Less-Common Met. 46 (1976) 39.
76W1 Will, G., Kossobutzki, K. H.: J. Less-Common Met. 47 (1976) 33.
76W2 Will, G., Kossobutzki, K. H.: J. Less-Common Met. 47 (1976) 43.
77B Berezin, A. A., Golikova, O. A., Zaitsev, V. R., Kazanin, M. M., Orlov, V. M., Tkalenko, E. N., in:Boron and Refractory Borides, (Matkovich V. 1., ed.) Springer: Berlin, Heidelberg, New York 1977, p. 52.
77M1 Makarenko, G. N.: see [77B], p. 310.
77M2 Matkovich, V. I., Economy, J.: see [77B], p. 96.
78H Haworth, D. T., Wilkie, C. A.: J. Inorg. Nucl. Chem. 40 (1978) 1689.
79B Binneabruck, H., Werheit, H.: Z. Naturforsch. 34a (1979) 787.
79K1 Kirfel, A., Gupta, A., Will, G.: Acta Crystallogr. B 35 (1979) 1052.
79K2 Kirfel, A., Gupta, A., Will, G.: Acta Crystallogr. B 35 (1979) 2291.
80K Kirfel, A., Will, G.: Acta Crystallogr. B 36 (1980) 1311.
81A Armstrong, D. R.: Proc. 7th Int. Symp. Boron, Borides and Related Compounds. Uppsala, Sweden, 1981; spec. issue of J. Less-Common Met. 82 (1981) 357.
81B1 Bouchacourt, M., Thevenot, F.: J. Less-Common Met. 82 (1981) 227 (Proc. 7th Int. Symp. Boron, Borides and Rel. Compounds, Uppsala, Sweden, 1981).
81B2 Bouchacourt, M., Thevenot, F.: see [81A], p. 227.
81S Schwetz, K. A., Reinmuth, K., Lipp, A.: Radex-Rundschau, 1981, 568.
81W Werheit, H., de Groot, K., Malkemper, W., Lundström, T.: see [81A1], p. 163.
86A Alexander, M.N.: in: Boron-Rich Solids (AIP Conf. Proc. 140), Albuquerque, New Mexico 1985, D. Emin, T.L. Aselage, C.L. Beckel, I.A. Howard ed., American Institute of Physics: New York, 1986, p. 168.
86B Bray, P.J.: in: Boron-Rich Solids (AIP Conf. Proc. 140), Albuquerque, New Mexico 1985, D. Emin, T.L. Aselage, C.L. Beckel, I.A. Howard ed., American Institute of Physics: New York, 1986, p. 142.
86C Conard, J., Bouchacourt, M., Thévenot, F.: J. Less-Common Met. 117 (1986) 51 (Proc. 8th Int. Symp. Boron, Borides, Carbides, Nitrides and Rel. Compounds, Tbilisi, Oct. 8 - 12, 1984).
86D Duncan, T.M.: in: Boron-Rich Solids (AIP Conf. Proc. 140), Albuquerque, New Mexico 1985, D. Emin, T.L. Aselage, C.L. Beckel, I.A. Howard ed., American Institute of Physics: New York, 1986, p. 177.
86L Larson, A.C.: in: Boron-Rich Solids (AIP Conf. Proc. 140), Albuquerque, New Mexico 1985, D. Emin, T.L. Aselage, C.L. Beckel, I.A. Howard ed., American Institute of Physics: New York, 1986, p. 109.
86M Mackinnon, I.D.R., Aselage, T., van Deusen, S.B.: in: Boron-Rich Solids (AIP Conf. Proc. 140), Albuquerque, New Mexico 1985, D. Emin, T.L. Aselage, C.L. Beckel, I.A. Howard ed., American Institute of Physics: New York, 1986, p. 114.
86W Will, G., Kirfel, A.: in: Boron-Rich Solids (AIP Conf. Proc. 140), Albuquerque, New Mexico 1985, D. Emin, T.L. Aselage, C.L. Beckel, I.A. Howard ed., American Institute of Physics: New York, 1986, p. 87.
86Y Yakel, H.L.: in: Boron-Rich Solids (AIP Conf. Proc. 140), Albuquerque, New Mexico 1985, D. Emin, T.L. Aselage, C.L. Beckel, I.A. Howard ed., American Institute of Physics: New York, 1986, p. 97.
87H Higashi, I., Ito, T.: in: Proc. 9th Int. Symp. Boron, Borides and Rel. Compounds, University of Duisburg, Germany, Sept. 21 - 25, 1987, H. Werheit ed., University of Duisburg: Duisburg, 1987, p. 41.
87L Lee, W.H., Shelton, R.N.: J. Low Temp. Phys. 68 (1987) 147.
87M Morosin, B., Aselage, T.L., Feigelson, R.S.: in: Novel Refractory Semiconductors, MRS Symp. Proc. Vol. 97, D. Emin, T.L. Aselage, C. Wood ed., Materials Research Soc.: Pittsburgh, 1987, p. 145.

91A Aselage, T.L., Emin, D.: in: Boron-Rich Solids, Proc. 10th Int. Symp. Boron, Borides and Rel. Compounds, Albuquerque, NM 1990 (AIP Conf. Proc. 231), D. Emin, T.L. Aselage, A.C. Switendick, B. Morosin, C.L. Beckel ed., American Institute of Physics: New York, 1991, p. 177.

91G Gosset, D., Colin, M.: J. Nucl. Mater. 183 (1991) 161.

91H Higashi, I., Kobayashi, M., Akagawa, Y., Kabayashi, K., Bernhard, J.: in: Boron-Rich Solids, Proc. 10th Int. Symp. Boron, Borides and Rel. Compounds, Albuquerque, NM 1990 (AIP Conf. Proc. 231), D. Emin, T.L. Aselage, A.C. Switendick, B. Morosin, C.L.Beckel ed., American Institute of Physics: New York, 1991, p. 224.

91K Kirkpatrick, R.J., Aselage, T., Phillips, B.L., Montez, B.: in: Boron-Rich Solids, Proc. 10th Int. Symp. Boron, Borides and Rel. Compounds, Albuquerque, NM 1990 (AIP Conf. Proc. 231), D. Emin, T.L. Aselage, A.C. Switendick, B. Morosin, C.L. Beckel ed., American Institute of Physics: New York, 1991, p. 261.

91L Lundström, T.: in: Boron-Rich Solids, Proc. 10th Int. Symp. Boron, Borides and Rel. Compounds, Albuquerque, NM 1990 (AIP Conf. Proc. 231), D. Emin, T.L. Aselage, A.C. Switendick, B. Morosin, C.L. Beckel ed., American Institute of Physics: New York, 1991, p. 186.

91M Morosin, B., Aselage, T.L., Emin, D.: in: Boron-Rich Solids, Proc. 10th Int. Symp. Boron, Borides and Rel. Compounds, Albuquerque, NM 1990 (AIP Conf. Proc. 231), D. Emin, T.L. Aselage, A.C. Switendick, B. Morosin, C.L. Beckel ed., American Institute of Physics: New York, 1991, p. 193.

92A1 Aselage, T.L., Tissot, R.G.: J. Am. Ceram. Soc. 75 (1992) 1052.

92A2 Aselage, T.L., Tissot, R.G.: J. Am. Ceram. Soc. 75 (1992) 2207.

92K1 Kuhlmann, U., Werheit, H., Schwetz, K.A.: J. Alloys Compounds 189 (1992) 249.

92K2 Kuhlmann, U., Werheit, H.: Solid State Commun. 83 (1992) 849.

94K1 Kuhlmann, U.: Zusammenhänge zwischen den Phononenspektren borreicher Festkörper mit Ikosaederstruktur und ihren strukturellen und elektronischen Eigenschaften, Thesis, Gerhard-Mercator University, Duisburg, Germany, 1994.

94K2 Kuhlmann, U., Werheit, H.: Proc. 11th Int. Symp. Boron, Borides and Rel. Compounds, Tsukuba, Japan, August 22 - 26, 1993, Jpn. J. Appl. Phys. Series 10 (1994), p. 84.

94K3 Kimura, K., Schmechel, R., Werheit, H.: unpublished (1994).

94L Lundström, T., Bolmgren, H.: Proc. 11th Int. Symp. Boron, Borides and Rel. Compounds, Tsukuba, Japan, August 22 - 26, 1993, Jpn. J. Appl. Phys. Series 10 (1994), p. 1.

94W1 Werheit, H., Kuhlmann, U., Lundström, T.: J. Alloys Compounds 204 (1994) 197.

94W2 Werheit, H., Kuhlmann, U., Lundström, T.: Proc. 11th Int. Symp. Boron, Borides and Rel. Compounds, Tsukuba, Japan, August 22 - 26, 1993, Jpn. J. Appl. Phys. Series 10 (1994), p. 5.

95M Morosin, B., Kwei, G.H., Lawson, A.C., Aselage, T.L., Emin, D.: J. Alloys Compounds 226 (1995) 121.

95N Nahm, K., Kim, C.K., Mittag, M., Jeong, Y.H.: J. Appl. Phys. 78 (1995) 3980.

96K1 Kasper, B.: (personal communication).

96K2 Kwei, G.H., Morosin, B.: J. Phys. Chem. 100 (1996) 8031.

98R Rogl, P.: in: Phase diagrams of ternary metal-boron-carbon systems, G. Effenberg ed., ASM International: Materials Park, OH, 1998.

99S1 Schmechel, R., Werheit, H.: J. Phys.: Condens. Matter 11 (1999) 6803.

99S2 Schmechel, R., Werheit, H.: J. Solid State Chem. (2000) (Proc. 13th Int. Symp. Boron, Borides and Rel. Compounds, Dinard, France, Sept. 1999: Structural defects of icosahedral boron-rich solids and their correlation with the electronic properties).

99W Werheit, H., Au, T., Schmechel, R., Shalamberidze, S.O., Kalandanze, G.I., Eristavi, A.M.: J. Solid State Chem. (2000) (Proc. 13th Int. Symp. Boron, Borides and Rel. Compounds, Dinard, France, Sept. 1999).

Fig. 1.

α-rhombohedral boron structure group, Unit cells of the α-rhombohedral boron structure family. **(a)** α-rhombohedral boron; **(b)** $B_{12}X_2$ structure; **(c)** $B_{12}X_3$ structure. Closed circles: polar atoms of the icosahedra forming covalent inter-icosahedral bonds; open circles: equatorial atoms of the icosahedra forming the weak three-center bonds in **(a)** and strong bonds to the chain end atoms of the chains in **(b)** and **(c)**.

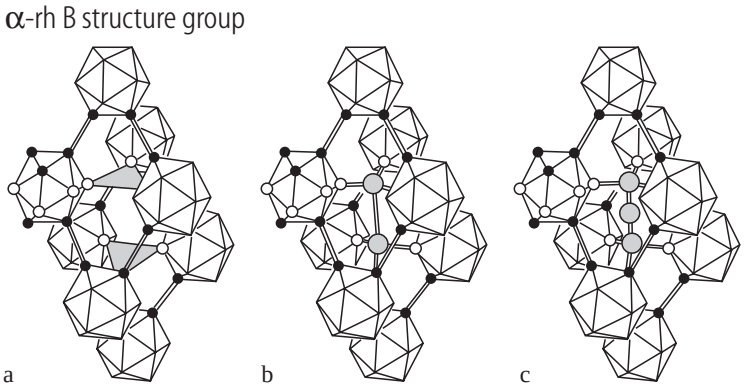

Fig. 2.

Boron carbide. Rhombohedral unit cell. Interatomic separations (in Å) determined from single crystal studies on boron carbide with carbon concentrations near 20 at. %, 16 at. % and 13.3 at. % (top to bottom). Icosahedra: open circles, equatorial sites; filled circles, polar sites [91A, 92A2].

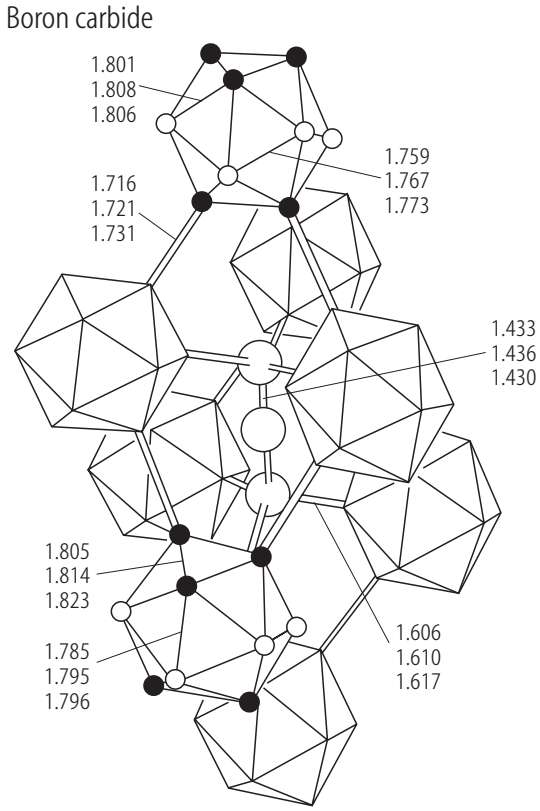

Fig. 3.

Boron carbide. a) C–B–C chain in the unit cell and the equatorial icosahedral B atoms to which it bonds. b) Planar B_4 group and the icosahedral atoms to which it bonds in one of six possible locations for the pair of B(6) atoms. c) Icosahedron with the atom positions to which the C–B–C chain (Fig. a) or the planar B_4 group (Fig. b) bonds [75Y].

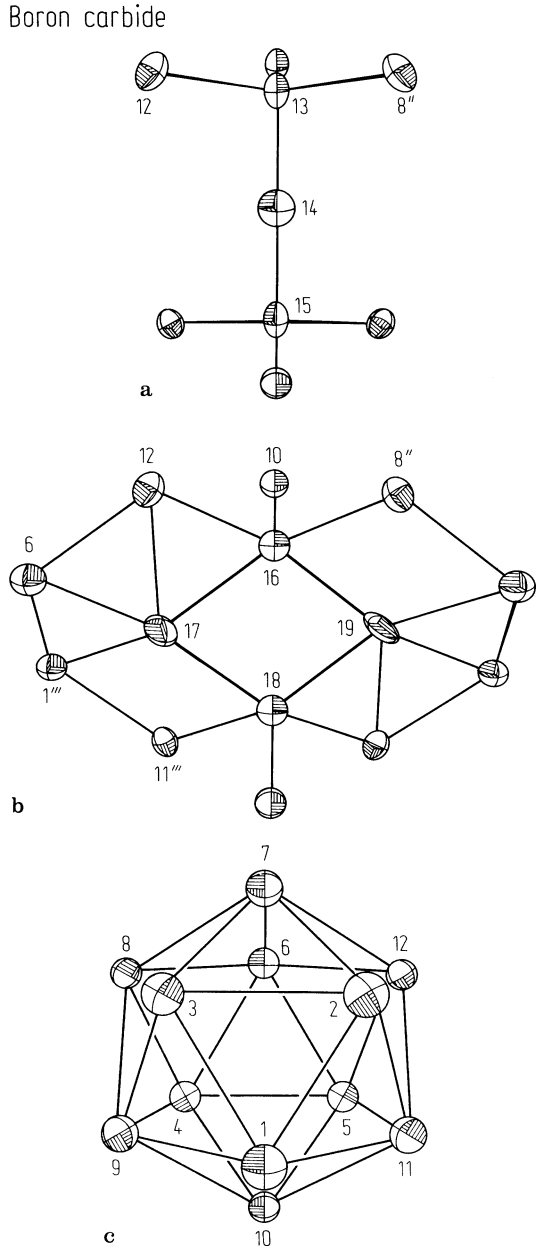

Fig. 4.

Boron carbide. **(a)** Density of atom arrangements on the trigonal axis of the rhombohedral unit cell of boron carbide (CBC and CBB chains, B□B arrangements); solid symbols [99S1, 99S2], open symbols, determined by phonon spectroscopy [92K1, 92K2]; diamonds, B(3) vacancies (center of the three-atom chain) determined by neutron scattering [96K2]. The reason for the considerable difference close to the boron-rich limit of the homogeneity range is that in the phonon spectroscopy the absolute oscillator strengths were used, while in [99S1, 99S2] their relation is taken and thus experimental error by light scattering at non-ideal surfaces was largely eliminated. Calculated valence electron deficiency for comparison. **(b)** Density of B_{12} and $B_{11}C$ icosahedra calculated from the densities of the atoms on the trigonal axis and the stoichiometry of the samples (for details see Tab. 1 in [92K1]); solid symbols, [99S1, 99S2], open symbols, determined by phonon spectroscopy [92K1, 92K2]. For the differences close to the carbon-rich limit of the homogeneity range see Fig. (a).

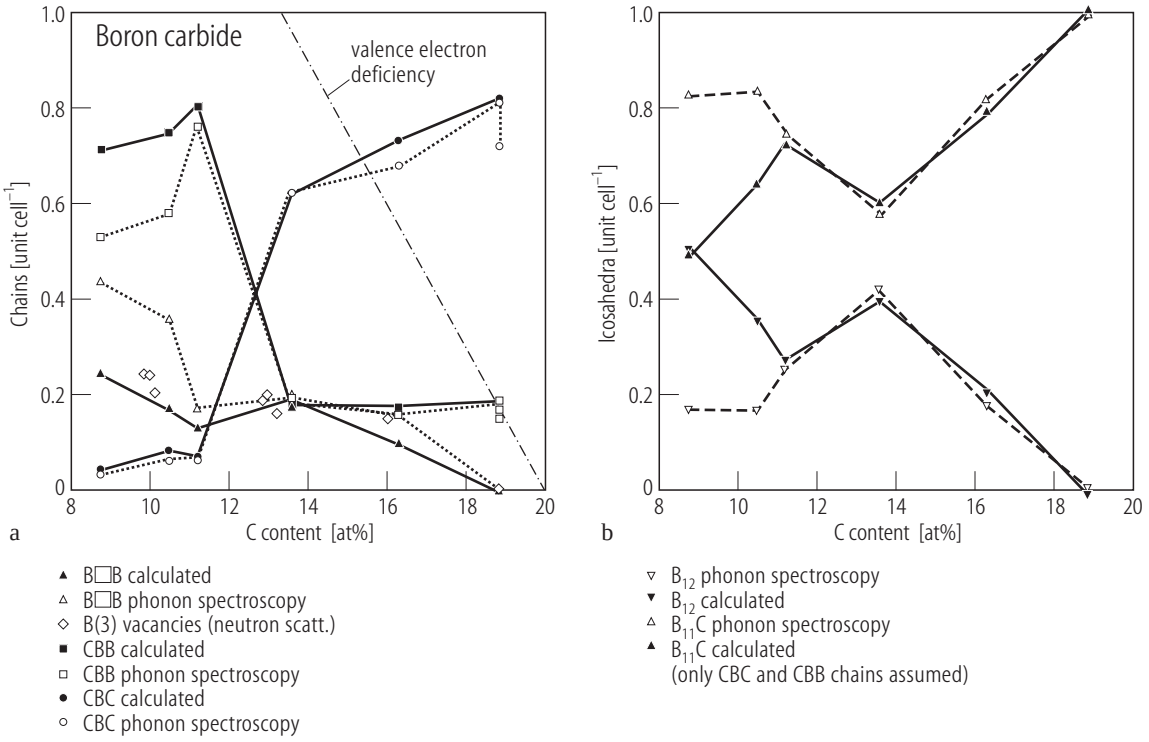

Fig. 5.

Boron carbide. **(a).** Concentration of CBC, CBB, CCC chains and B□B arrangements on the trigonal axis per unit cell vs. C content. Full lines connecting full symbols, results based on the averaged CCC concentrations determined for the isotope enriched samples [99S2, 99W]. Dashed lines connecting open symbols, results based on the measured oscillator strengths of the additional chain phonon obtained from [92K1, 92K2, 94K1]; diamonds: B(3) vacancies determined by neutron scattering [96K2].**(b)** Concentrations of B_{12} and $B_{11}C$ icosahedra vs. C content. Full symbols, based on the averaged concentration of CCC chains (see Fig. **(a)**; open symbols, based on the measured oscillator strengths of the additional chain phonon obtained from [92K1, 92K2, 94K1].

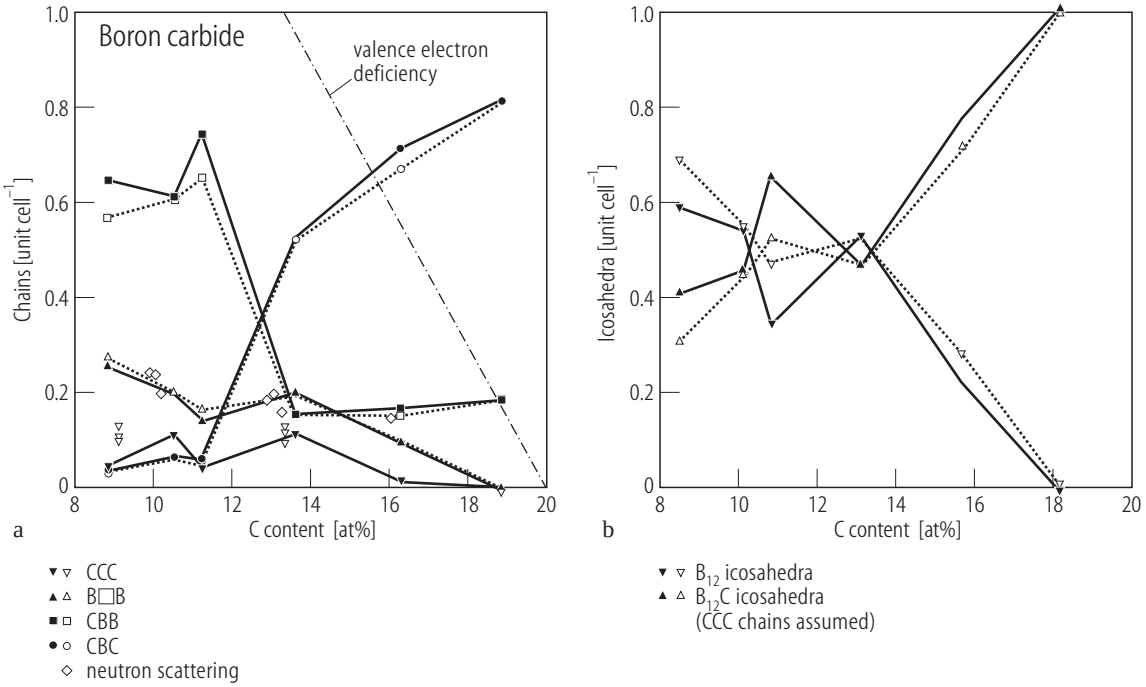

Fig. 6.

Boron carbide. Vacancy-interstitial pair occupancies (interstitial B(6) site away from the chain center B(3)) vs. carbon concentration. Different symbols distinguish between samples prepared at different times [95M].

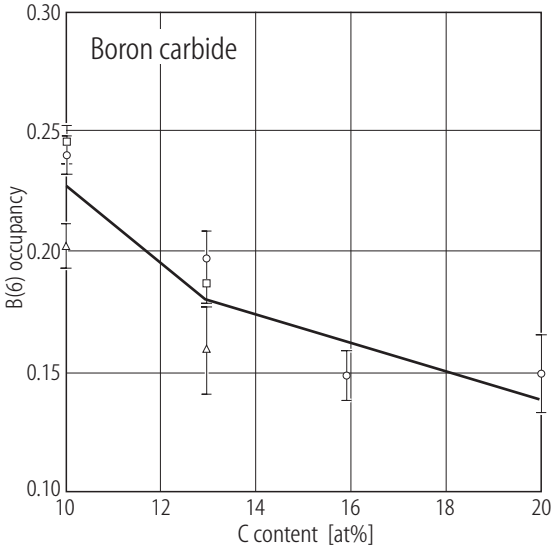

Fig. 7.

Boron carbide. Rhombohedral unit cell. Interatomic separations (in Å) determined from single crystal studies on boron carbide with carbon concentrations near 20 at. %, 16 at. % and 13.3 at. % (top to bottom). Icosahedra: open circles, equatorial sites; filled circles, polar sites [91A, 92A2].

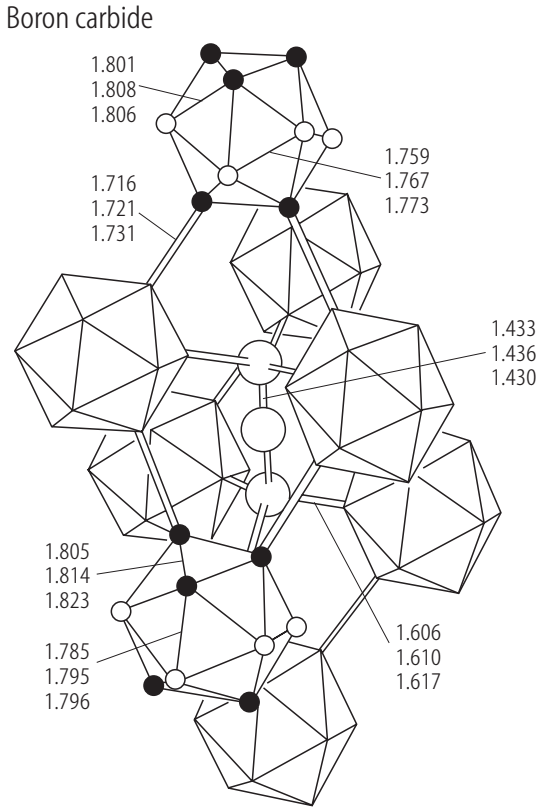

Fig. 8.

Boron carbide. Arrangement of the atoms in the unit cell. White balls: atoms of the icosahedra located on the edges of the unit cell; grey balls: equatorial atoms of the icosahedra forming multiple-center bonds; black balls: atoms of the three–atomic linear C–B–C chain; (cp. e.g. [66S, 79B, 81S]).

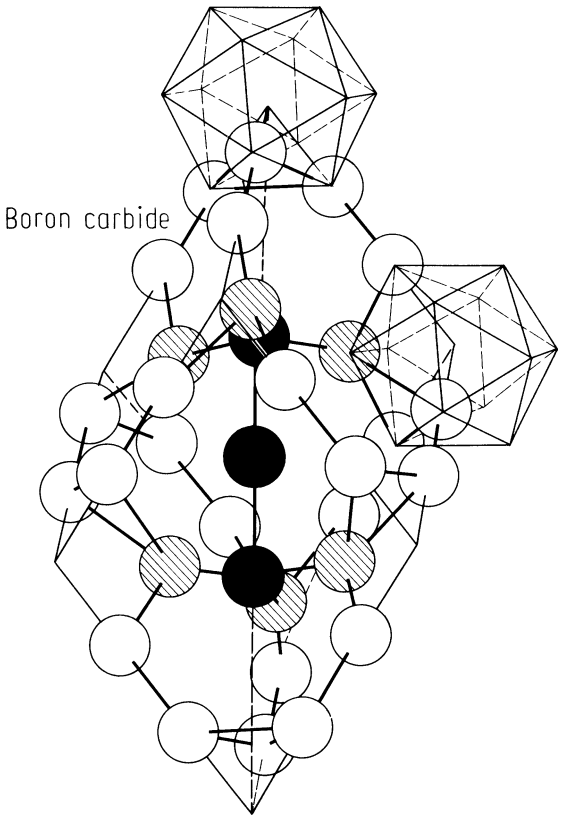

Fig. 9.

Boron carbide. Room temperature rhombohedral lattice parameters vs. carbon content a) according to [75Y] (see also [71K]) (expected errors in the compositions: +1%); b) according to [81B1.

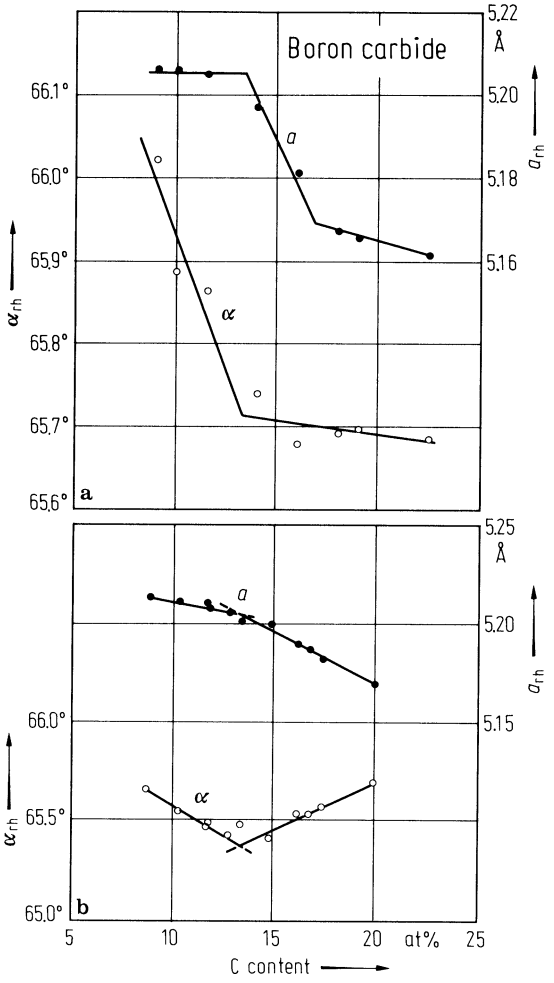

Fig. 10.

Boron carbide. Lattice parameters *a*, *c* (in hexagonal representation) vs. carbon content. Bars, standard errors for 90 % confidence [91G].

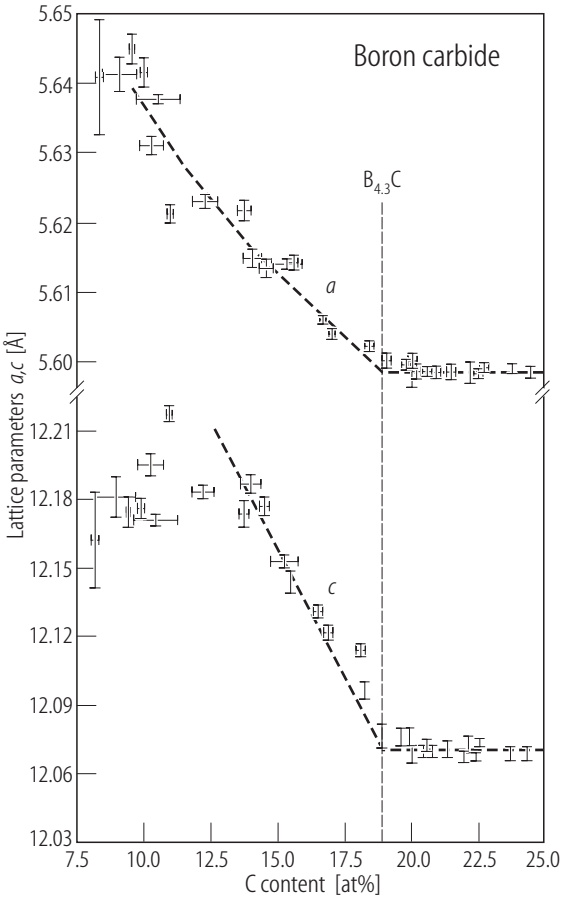

Fig. 11.

Boron carbide. Lattice parameters a, α (in rhombohedral representation) vs. carbon content. Bars, standard errors for 90 % confidence. [91G].

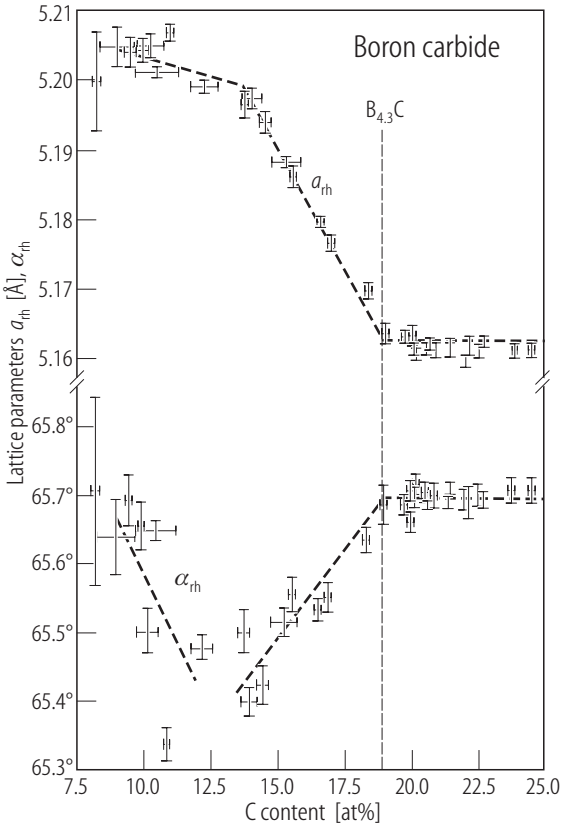

Fig. 12.

Boron carbide. Volume of the rhombohedral unit cell vs. carbon content. Data points with straight line bars for standard errors with 90 % confidence [91G]. Full line [81B1].

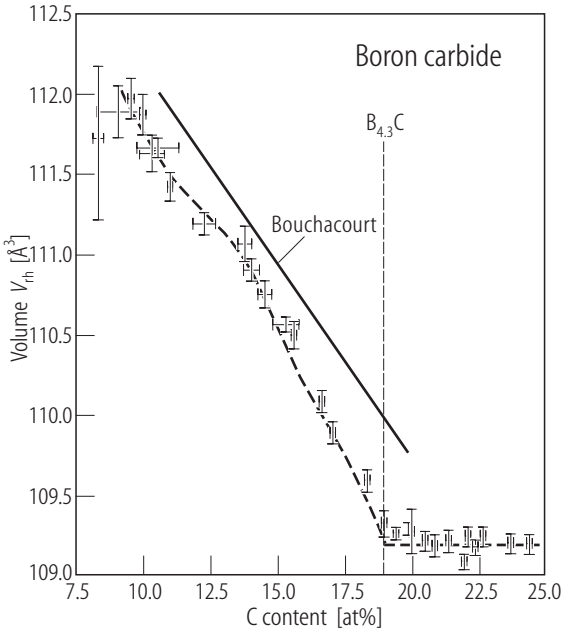

Fig. 13.

Boron carbide. Pressure dependence of the relative volumes (V/V_0) of the unit cell (open symbols) and the icosahedral volume (solid symbols). The different symbols represent the data obtained on different samples; The solid, dashed and dotted lines represent linear fits to the behavior of icosahedra, unit cell and intericosahedral space [95N].

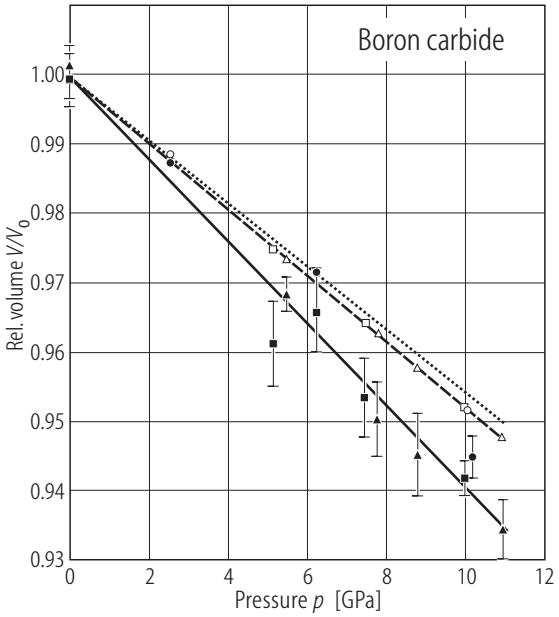

Fig. 14.

Boron carbide. „Thermal factors“ along **(a)** the basal plane, U_{11}, and **(b)** the *c* axis, U_{33}, vs. C concentration obtained from single crystal X-ray refinements. Open circles, B(1) site; full triangles, B(2) site; full circles, B(3) site; open triangles, C site [91A]. The "thermal factors" contain the thermal vibration of atoms and the variation of atomic positions in differently composed elementary cells as well.

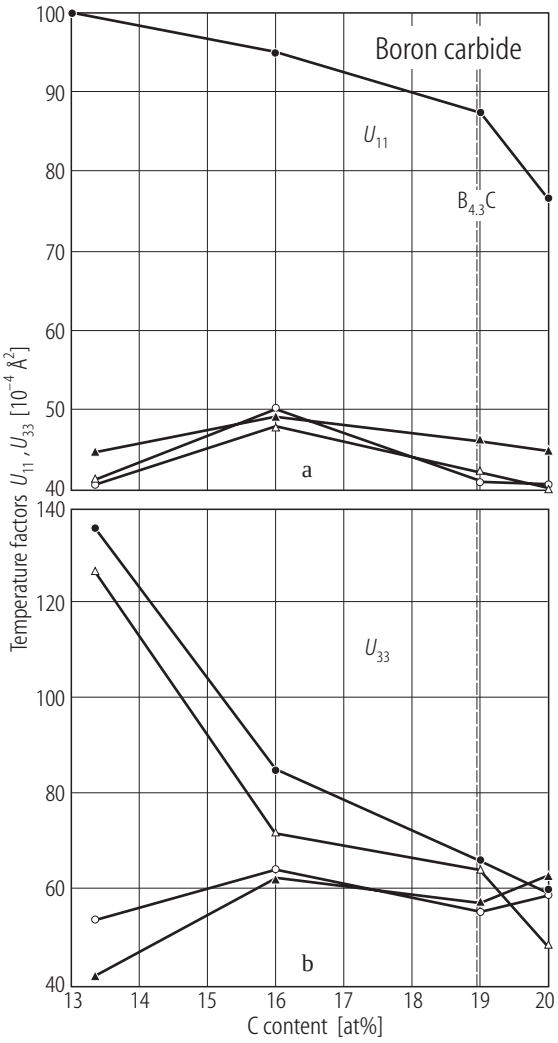

Fig. 15.

Boron carbide. Compositional variation of ^{13}C and ^{11}B MAS NMR chemical shifts and peak widths [91K]. (MAS: magic-angle spinning).